Post-Caledonian extension in the West Norway–northern North Sea region: the role of structural inheritance

HAAKON FOSSEN[1,2]*, HAMED FAZLI KHANI[1], JAN INGE FALEIDE[3], ANNA K. KSIENZYK[1] & W. JAMES DUNLAP[4]

[1]*Department of Earth Science, University of Bergen, Postboks 7803, 5007 Bergen, Norway*

[2]*Museum of Natural History, University of Bergen, Postboks 7803, 5007 Bergen, Norway*

[3]*Department of Geosciences, University of Oslo, Postboks 1047, Blindern, N-0316 Oslo, Norway*

[4]*University Gas Research, 2888 Pelican Point Circle, Mound, MN 55364, USA*

**Corresponding author (e-mail: haakon.fossen@geo.uib.no)*

Abstract: The northern North Sea region has experienced repeated phases of post-Caledonian extension, starting with extensional reactivation of the low-angle basal Caledonian thrust zone, then the formation of Devonian extensional shear zones with 10–100 km-scale displacements, followed by brittle reactivation and the creation of a plethora of extensional faults. The North Sea Rift-related approximately east–west extension created a new set of rift-parallel faults that cut across less favourably orientated pre-rift structures. Nevertheless, fault rock dating shows that onshore faults and shear zones of different orientations were active throughout the history of rifting. Several of the reactivated major Devonian extensional structures can be extrapolated offshore into the rift, where they appear as bands of dipping reflectors. They coincide with large-scale boundaries separating 50–100 km-wide rift domains of internally uniform fault patterns. Major north–south-trending rift faults, such as the Øygarden Fault System, bend or terminate against these boundaries, clearly influenced by their presence during rifting. Hence, the North Sea is one of several examples where pre-rift basement structures oblique to the rift extension direction can significantly influence rift architecture, even if most of the rift faults are newly-formed structures.

Rifts and regions of extensional tectonics are built on crust that has undergone earlier phases of deformation, particularly orogenic events (Wilson 1966). Hence, abundant pre-existing structures generally exist in regions where rifting initiates, but the role of such structures during rifting and extension has been a long-standing question in the geoscience community. Reactivation of both low-angle thrusts (e.g. Brewer & Smythe 1984; Constenius 1996) and high-angle normal faults (e.g. Henza *et al.* 2011; Bell *et al.* 2014) has been reported, and several studies argue that major pre-existing structures may give rise to rift segmentation and the formation of transfer zones or fault-domain boundaries (Rosendahl *et al.* 1986; Morley *et al.* 1990, 2004; Faulds & Varga 1998).

The northern North Sea rift system and its margins (Fig. 1) constitute an area that has been subjected to not only Caledonian thrusting, but several phases of extensional deformation since the end of the Caledonian continent–continent collision at around 405 Ma, notably post-collisional (Devonian) crustal extension, and two main phases of North Sea rifting in the Permian–Early Triassic and Late Jurassic–Early Cretaceous (Phase 1 and Phase 2, respectively). The Caledonian collision resulted in a highly heterogeneous crust with a structural imprint expressed in the form of lithological layering, mylonitic fabrics, shear zones and thrusts in the lower and middle Caledonian crust, as well as brittle thrusts and normal faults in the, now mostly removed, upper Caledonian crust. Such an anisotropic crust, with a substantial assembly of potentially weak structures, is likely to respond to later extensional deformation by a certain amount of reactivation, depending on factors such as geometry, dip, orientation relative to the extension direction and relative strength.

In this work, we combine new and existing observations and data to demonstrate that the onshore extensional shear zones, faults and fractures show evidence of extensional activation both before and during the rift history of the northern North Sea, and seismic data to argue that post-Caledonian extensional structures were also reactivated during rifting, and that they had a significant influence on the first-order architecture of the rift system.

Caledonian framework

The Caledonian orogen has been the subject of numerous studies since the 1800s, with a strong

From: Childs, C., Holdsworth, R. E., Jackson, C. A.-L., Manzocchi, T., Walsh, J. J. & Yielding, G. (eds) *The Geometry and Growth of Normal Faults*. Geological Society, London, Special Publications, **439**, http://doi.org/10.1144/SP439.6

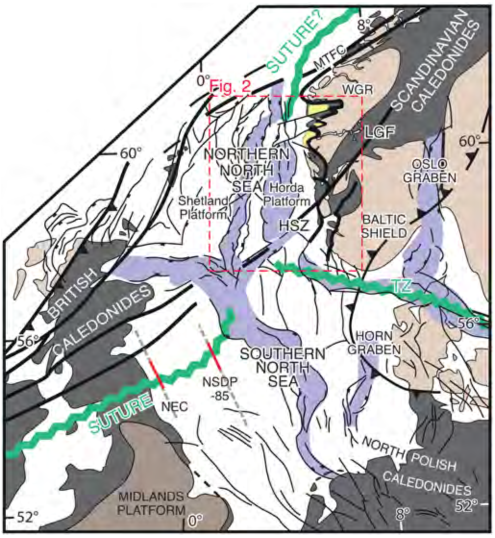

Fig. 1. Geological setting of the North Sea area, with the study area outlined. NEC and NSDP are deep seismic lines from which the Caledonian suture is interpreted (from Freeman *et al.* 1988). HSZ, Hardangerfjord Shear Zone; LGF, Lærdal–Gjende Fault; MTFC, Møre–Trøndelag Fault Complex; TZ, Tornquist Zone; WGR, Western Gneiss Region. Note that the precise location of the suture zone is not known offshore Norway.

focus on the accretional (collisional) part of the Caledonian evolution. Only relatively recently has it become clear that post-collisional Devonian extensional deformation had a profound impact on the Scandinavian Caledonides (Fossen 2010 and references therein), and that this pre-rift extension created a structural framework that must have influenced the formation and evolution of the Permian–late Jurassic North Sea Rift, as discussed in this contribution.

The extensional history explored here initiates with the termination of the main and final collisional phase of the Caledonian orogenic evolution, known as the Scandian Phase (or Scandian Orogeny) (e.g. Gee *et al.* 2008). The Scandian Phase is explained as a continent–continent collision that lasted from approximately 425 to 405 Ma, resulting in subduction of the western margin of Baltica underneath the Laurentian lithospheric plate, and the creation of an associated asymmetric orogenic edifice consisting of a Baltican pro-wedge of continental and oceanic allochthonous units and a somewhat smaller retro-wedge on the Laurentian margin. This interpretation is based on the general northwestwards increase in Caledonian temperature (T) and pressure (P) estimates in the Baltican basement, notably in the Western Gneiss Region (WGR) of SW Norway, where late Caledonian P–T estimates of more than 36 GPa–800°C have been reported from the northwestern parts (Smith & Lappin 1989; Dobrzhinetskaya *et al.* 1995; Wain 1997; Hacker *et al.* 2010). These observations place the Caledonian (or Iapetus) suture zone west of the current Norwegian coastline (Fig. 1).

The pro-wedge of allochthonous units (thrust nappes) and the underlying Baltican basement were separated by a regionally significant basal thrust or décollement zone (Fig. 2) (Fossen 1992; Milnes *et al.* 1997). Internally, the orogenic wedge contains a number of large and small thrust nappes and related thrusts, where the upper tectonic units in Scandinavia have been translated several hundred kilometres to the SE (e.g. Hossack & Cooper 1986), with complementary NW-directed thrusting in the Scottish Caledonides (retro-wedge) (e.g. Butler 2010). Hence, the Caledonian collisional phase left a highly heterogeneous crust at the dawn of a prolonged history of post-Caledonian extensional deformation, with an important large-scale three-layer rheological stratification in the Scandinavian Caledonides composed of a strong Baltican basement, a basal thrust zone comprising mainly weak micaceous metasediments, and allochthons of strong Precambrian continental crust (continental nappes in Fig. 2). The suture zone, which is the zone of oceanic terrane(s) separating Laurentian from Baltican or, to the south, Avalonian lithosphere, is interpreted to be represented by a band of north-dipping reflections on deep seismic data of the BIRPS project, acquired in the 1980s (Klemperer & Matthews 1987; Freeman *et al.* 1988). These deep seismic lines suggest that the suture extends to the NE into the northern North Sea Rift, more or less in the direction of the Hardangerfjord Shear Zone (Fig. 1). However, off the coast of Norway, the deep seismic coast-parallel ILP lines (see Fig. 2 for location) show a south-dipping mantle shear zone that offsets the Moho in a normal sense: that is, the opposite of what we would expect for a subduction-related Caledonian feature (Gabrielsen *et al.* 2015) (Fig. 3). Furthermore, the isotherms and isobars related to the Scandian collision in South Norway in general, and the WGR basement in particular, show that the suture zone must turn northwards more or less parallel to the trend of the Viking Graben–Sogn Graben. However, a mantle feature similar to that interpreted as the suture across the British Isles has not been found on deep seismic lines crossing the northern North Sea, except perhaps for east-dipping reflections on line NSDP84-1 that appear to be an extensional structure (Gibbs 1987; Odinsen *et al.* 2000). The reason for its absence on deep seismic lines may be the profound post-collisional extensional reworking in this part of the orogen.

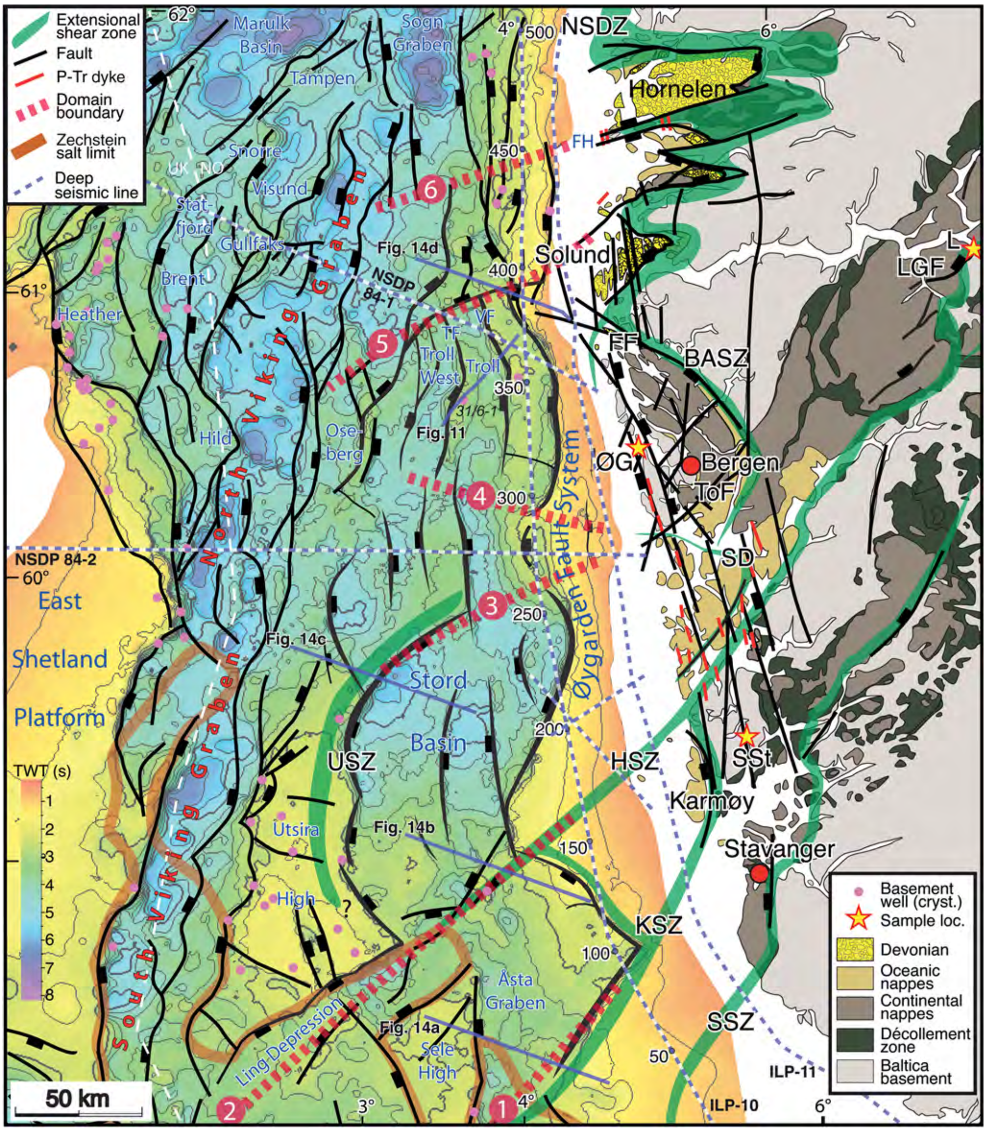

Fig. 2. Onshore–offshore map of the northern North Sea Rift (the area outlined in Fig. 1). Major onshore Devonian extensional shear zones are extended into the rift where observed on seismic sections. The fault pattern of the rift is shown over a top basement map, where anything older than Permian is considered basement. FF, Fensfjord Fault; FH, Florø Horst; SSZ, KSZ, HSZ and BASZ, Stavanger, Karmøy, Hardangerfjord and Bergen Arcs shear zones; NSDZ, Nordfjord–Sogn Detachment Zone; LGF, Lærdal–Gjende Fault; SD, Sunhordland Detachment; TF, Tusse Fault; ToF, Totland Fault; USZ, Utsira Shear Zone; VF, Vette Fault; P–Tr, Permo-Triassic. Wells drilled to crystalline basement are from Bassett (2003). Starred localities are tagged with letters referred to in the text.

Devonian extension of Caledonian crust

Reactivation of the low-angle basal Caledonian thrust zone (Mode I extension)

The numerous hinterland-dipping Caledonian thrusts and shear zones in the lower Devonian crust in South Norway were clearly prone to reactivate as the tectonic regime changed from one of regional contraction to extension. The current erosion level exposes the Caledonian basal thrust or décollement zone particularly well, and field studies show that, although this zone was the basal thrust of the Caledonian orogenic wedge, it is completely

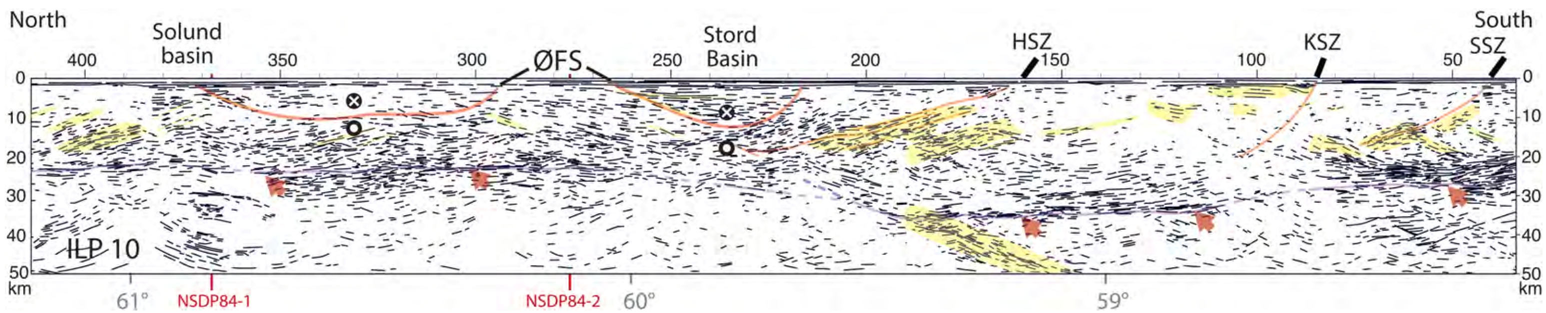

Fig. 3. Line drawing of deep seismic line ILP-10. See Figure 2 for the location and Gabrielsen *et al.* (2015) for detailed information. Some dipping domains are outlined, and arrows indicate the location of the Moho. ØFS, Øygarden Fault System, which is transected along-strike. See the caption to Figure 2 for more abbreviations.

dominated by top-to-hinterland (NW) kinematic indicators that formed during extensional reactivation of the low-angle basal Caledonian décollement zone (Mode I extension: Fossen 1992; Fossen & Dunlap 1998). Interestingly, the extensional reactivation occurred while this zone was a very low-angle structure with an estimated northwesterly dip in the eastern and central part of only 3–5°, steepening to the NW (Fossen 2000). The reactivation of this low-angle basal décollement zone in extension was facilitated by the strong contrast between its weak metasedimentary rocks (micaschists, phyllites and shales) and the much stronger underlying Proterozoic basement rocks and overlying crystalline basement nappes. Most likely, the expulsion of fluids released due to metamorphic reactions within the basal décollement zone also contributed to its weak nature. Ar/Ar ages of micas from the basal thrust zone suggest that the kinematic signature of this zone changed between 408 and 402 Ma (Fossen & Dunlap 1998). At this point, it turned into a low-angle extensional detachment on which the Caledonian orogenic wedge was translated toward the (north)west or, depending on our frame of reference, the motion of the Baltic Shield was reversed by motion towards the SE (eduction).

Secondary (Mode II) extensional shear zones

As displacement accumulated on the extensional low-angle Caledonian décollement zone, differential exhumation (more rapid exhumation in the hinterland) lowered its dip to the point where continued shearing became mechanically unfeasible (Nur *et al.* 1986). From that point on, continued extension was taken up by a set of new and steeper shear zones that transected the inactivated décollement zone. Most of these are NW- and west-dipping structures (Mode II extension: Fossen 1992) with up to several tens of kilometres of displacement. These shear zones segmented the Caledonian crust into major blocks that rotated to become foreland dipping (Fig. 3). The most impressive example of these Mode II shear zones is probably the strongly corrugated Nordfjord–Sogn Detachment Zone (NSDZ in Fig. 2), which, together with the steeper Bergen Arcs Shear Zone to the south, forms a close to 200 km-long detachment zone. The Nordfjord–Sogn Detachment Zone is probably connected to the NE-trending Møre–Trøndelag Fault Complex immediately north of the area covered by Figure 2 (MTFC in Fig. 1). South of the Bergen Arcs Shear Zone is the much straighter Hardangerfjord Shear Zone, and then the (again) curved Karmøy and Stavanger shear zones (KSZ and SSZ in Fig. 2). These shear zones are steeper than the basal décollement zone, from approximately 60° for the Bergen Arcs Shear Zone via the somewhat more gentle-dipping Karmøy Shear Zone and the approximately 25° Hardangerfjord Shear Zone to the folded but, in the extension direction, very-low-angle (5–10°) Nordfjord–Sogn Detachment Zone (Fig. 3).

The Nordfjord–Sogn Detachment Zone is defined by an up to 5–6 km-thick package of mylonites with abundant kinematic structures showing consistent normal (top-to-the-west) sense of shear. Its strongly mylonitic fabrics suggest displacements in excess of 50–100 km (Norton 1987; Andersen & Jamtveit 1990; Fossen 2000), as does the fact that the low-angle Nordfjord–Sogn Detachment Zone brings high-pressure rocks of the WGR in close contact with hanging-wall Devonian basins and low-grade Caledonian allochthonous units. An interesting and important feature of the Nordfjord–Sogn Detachment Zone is its folding about gently west-plunging axes, with subvertical axial surfaces (Chauvet & Séranne 1994; Krabbendam & Dewey 1998) (Fig. 4). This upright folding occurred before, during and after deposition of the preserved level of Devonian sediments, and is interpreted as a result of transtension associated with sinistral shear along the Møre–Trøndelag Shear Zone – the ductile precursor of the Møre–Trøndelag Fault Complex (Krabbendam & Dewey 1998). For the Hornelen Devonian basin area, the folding is tightest along the northern and southern margins, where mylonites and protomylonites of the Nordfjord–Sogn Detachment Zone define domains of steep dips to the north and south that, from a mechanical point of view, are easier to reactivate in the brittle regime than the shallowly dipping parts of the detachment zone.

The Hardangerfjord Shear Zone is perhaps the longest of the Mode II shear zones, with a minimum onshore length of 350 km, but with a maximum displacement of only about 10–15 km (Fossen & Hurich 2005). Its extension into the North Sea has been confirmed by deep seismic lines immediately offshore, where it appears as a NW-dipping band of reflectors that reaches the lower crust (Fig. 3) (Hurich & Kristoffersen 1988; Fossen & Hurich 2005; Gabrielsen *et al.* 2015).

Most or all of these oblique extensional shear zones probably reached, directly or indirectly, the surface as brittle fault zones, generating a system of Devonian continental basins. Much of the basin-fill has been removed by erosion, but the lower parts of four linked basins remain in the hanging wall of the Nordfjord–Sogn Detachment Zone in West Norway. These basins show stacking geometries (Steel *et al.* 1985) and palaeo-thermal structures (Fauconnier *et al.* 2014) that are consistent with a listric fault or supra-detachment model (Hossack 1984; Séranne & Séguret 1987) (Fig. 5), possibly with an influence of strike-slip tectonics

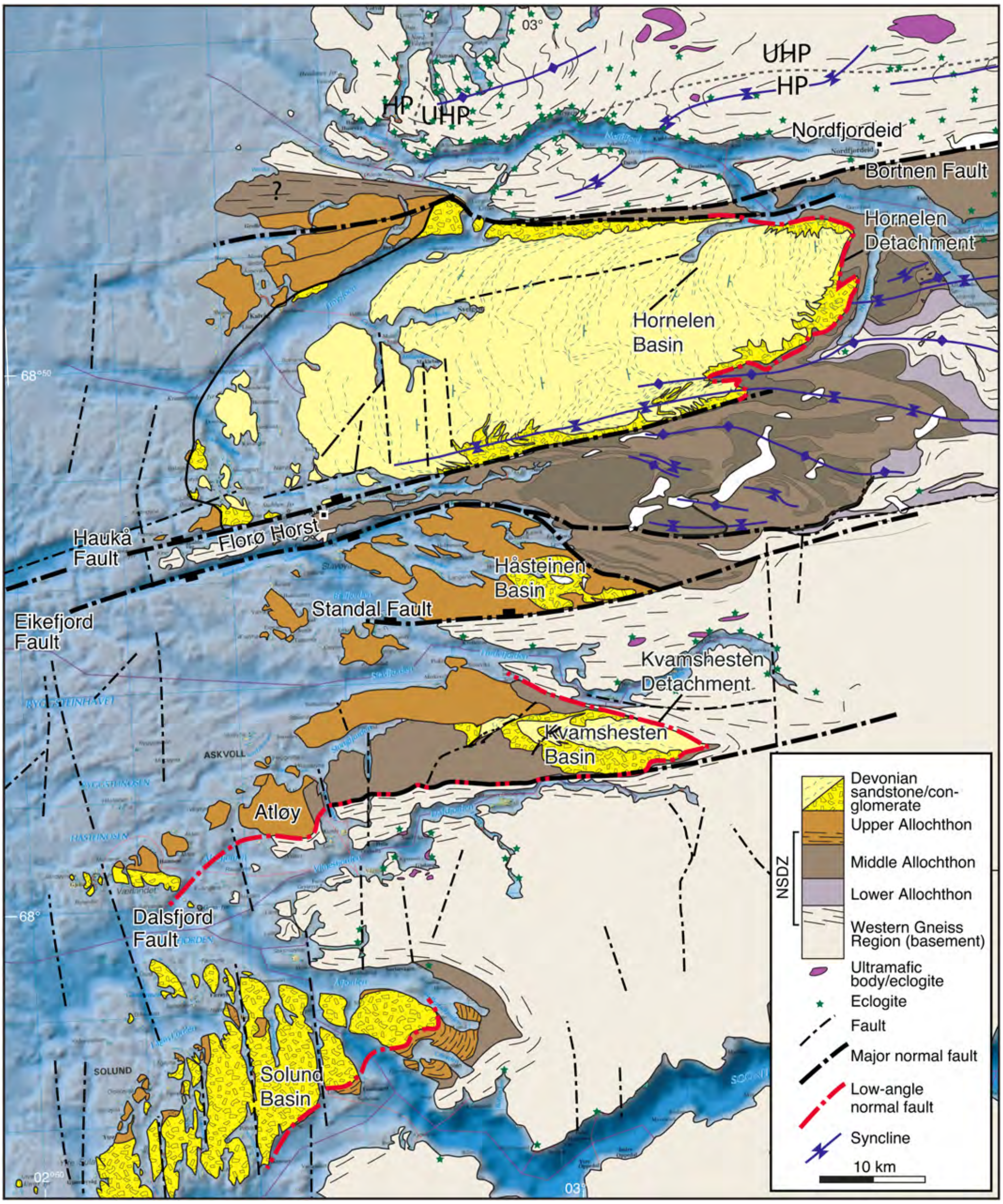

Fig. 4. Map of the area of Devonian basins in West Norway. Note the presence of low-angle normal faults (red), steeper WSW–ENE faults and sets of coast-parallel faults.

(Steel *et al.* 1985). For the Hornelen Basin, >25 km of stratigraphic thickness accumulated on top of the detachment system, while the maximum burial temperature seems to be more or less the same from the top to the bottom of the basin (i.e. from the western unconformity to the eastern end of the section shown in Fig. 5). This observation is consistent with the supra-detachment model, where repeated translation of the hanging wall on a low-angle detachment produced the accommodation space needed to create a stratigraphic thickness that almost tripled the true depth of the basin. A Middle Devonian (393–383 Ma) age of the upper part of the Hornelen Basin (Høeg 1945) shows that the basin

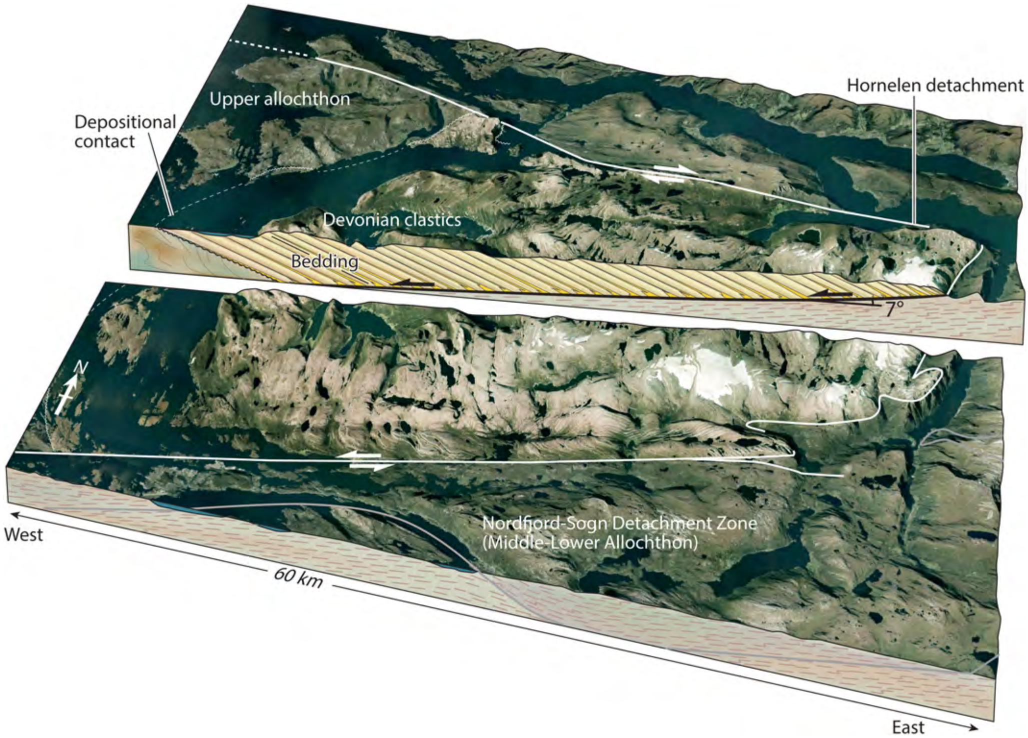

Fig. 5. 3D model of the Hornelen Basin resting on a brittle detachment against the mylonitic Nordfjord–Sogn Detachment Zone.

developed during the Devonian extensional shearing on the Nordfjord–Sogn Detachment Zone, which is indirectly dated by white mica cooling ages in the Western Gneiss Complex that range from 400 Ma in the SE part to 380 Ma in the NW part (Hacker 2007 and references therein). Hence, at the time of Devonian basin formation, the Nordfjord–Sogn Detachment Zone had already been exhumed to lower-amphibolite or greenschist facies conditions due to tectonic thinning and rotation of the WGR during the Mode II extension.

Brittle onshore faults

Reactivation of low-angle Devonian extensional shear zones

The vast majority of the oblique (Mode II) extensional shear zones described above were established as ductile (plastic) structures, but contain brittle elements such as the Hornelen Detachment (Fig. 4), the Dalsfjord Fault (Eide *et al.* 1997), the Lærdal–Gjende Fault (Andersen *et al.* 1999) and the Fensfjorden Fault (Wennberg *et al.* 1998) (FF in Fig. 2) that suggest extensional reactivation in the brittle regime (see later). These brittle elements are faults that are much thinner than the wide ductile shear zones in which they are located, and typically show evidence of multiphase evolution. Two of these have been subjected to palaeomagnetic and radiometric age determinations, and will be briefly discussed here.

The Lærdal–Gjende Fault (LGF in Figs 1 & 2) is a low-angle normal fault dipping 15–35° to the NW, located within the much broader and ductile low-angle (25°) Hardangerfjord Shear Zone (Fossen & Hurich 2005). The Lærdal–Gjende Fault is a composite brittle structure consisting of up to several hundred metres of cohesive greenish cataclasite that, as seen at the exceptionally well-exposed fault location in Lærdal (starred locality L in Fig. 2), contains 1–2 m-thick zone of non-cohesive fault gouge. The Lærdal–Gjende Fault omits the décollement (phyllite/micaschist) that acted as the basal thrust during Caledonian collision and as an extensional décollement during the subsequent Devonian extensional history (Lutro & Tveten 1996). In contrast, the Hardangerfjord Shear Zone is a ductile shear zone that preserves layer continuity across the zone. Hence, the Lærdal–Gjende Fault is an expression of brittle deformation along the ductile Devonian Hardangerfjord Shear Zone, possibly formed by brittle deformation of the feldspar-rich Jotun Nappe during Devonian cooling, but certainly active at later stages at low temperatures.

Andersen *et al.* (1999) applied palaeomagnetic dating methods to plugs from the greenish epidote-rich cataclasite zone of the Lærdal–Gjende Fault at the Lærdal locality to estimate activity on this fault, obtaining Permian and late Jurassic–early Cretaceous signatures that they interpreted as times of fault activity. More recently, we collected clay-rich fault gouge samples at the same locality (L in Fig. 2) that yielded a strong late Jurassic–early Cretaceous K–Ar signature (see later). This is in agreement with the fact that it was sampled from the non-cohesive part of the fault, which is generally considered to be the most recently active part of the fault. Hence, there is strong evidence for brittle reactivation of the low-angle Lærdal–Gjende Fault at the time of rifting in the North Sea and the Oslo Rift (see below).

The Dalsfjord Fault (Fig. 4) is a low-angle fault that marks the contact between the Devonian Kvamshesten Basin and the mylonitic middle allochthonous rocks of the Nordfjord–Sogn Detachment Zone (Osmundsen & Andersen 2001). The fault is well exposed at a locality in Atløy (Fig. 4), where a greenish cataclasite, quite similar to the one observed along the Lærdal–Gjende Fault, is post-dated by red breccia. A similar sequence of events as that documented from the Lærdal–Gjende Fault is observed through a combination of palaeomagnetic and Ar/Ar dating of its fault rocks: a strong late Permian signature overprinted by a late Jurassic–early Cretaceous event (Eide *et al.* 1997). This west-dipping low-angle fault shares similarities with the Hornelen Detachment. This detachment is another low-angle fault consisting of green flinty epidote-bearing cataclasite that shows evidence of later microfracturing (reactivation), defining the gently west-dipping tectonic contact between the Hornelen Basin and its mylonitic substrate (Nordfjord–Sogn Detachment Zone) (Figs 4 & 5). The Hornelen Detachment juxtaposed the Devonian basin with the top-to the-west mylonites of the Nordfjord–Sogn Detachment Zone, and the distribution of alluvial fans along the margins of the Hornelen Basin shows that it closely follows the original basin-forming fault.

It is an important observation that onshore low-angle Devonian extensional structures were reactivated as low-angle normal faults during the late Palaeozoic–Mesozoic rift history. Indeed, if such Devonian extensional shear zones are reactivated onshore, they are also likely to be reactivated offshore in the northern North Sea rift where rift-related strains are much higher.

Steeper faults associated with the Devonian basins

The Hornelen detachment serves as a good example of a very low-angle brittle fault truncated by steeper faults. In this case, steeper faults with ENE–WSW orientations are located along the north and south margins of the Hornelen Basin. The fault on the north side (the Bortnen Fault) is dipping steeply to the south, while the southern fault (the Haukå Fault) is dipping to the NNW. The Bortnen Fault is reported to show a sinistral sense of shear, with a subordinate normal component, and K-feldspar–epidote alteration, breccia and pseudotachylite as characteristic elements (Young *et al.* 2011). The marginal fan architecture of the Hornelen Basin shows that the Bortnen Fault closely approximates the locations of the original (synsedimentary) fault along the northern basin margin (Steel *et al.* 1985).

The southern (Haukå) marginal fault transects the Hornelen Detachment in the SE corner of the basin, where its normal offset can be demonstrated to exceed 500 m (Braathen 1999). Also, this fault closely corresponds to the syndepositional fault along the southern margin of the Hornelen Basin, as seen from the preserved marginal fan complex along the fault.

Together with the next major steep fault to the south (the Eikefjord Fault), the Haukå Fault defines a major NNE-trending horst structure that narrows down to a 4–5 km-wide structure towards the coast, here named the Florø Horst. In the western coastal part, the Florø Horst brings up gneisses interpreted to be part of the WGR (Lutro & Bryhni 2000), and places them in fault contact with upper allochthonous units both to the north (Haukå Fault) and to the south (Eikefjord Fault) (Fig. 4), suggesting several kilometres of displacement across both faults. Furthermore, the displacement increases to the west, suggesting that the horst structure and its associated faults stretch well into the northern North Sea rift basin.

General pattern of onshore faults and fracture zones

In general, a large population of brittle faults and fractures dissect the bedrock surface of SW Norway (Fig. 6), and the wide range in orientation suggests that they formed during more than one phase of deformation. The majority of the onshore brittle structures in the area covered by Figure 6 are post-lower Devonian faults that affect Caledonian and extensional lower Devonian ductile fabrics. However, Proterozoic elements are probably present in much of the Proterozoic basement SE of the Hardangerfjord Shear Zone, where the basement is generally unaffected by Caledonian deformation.

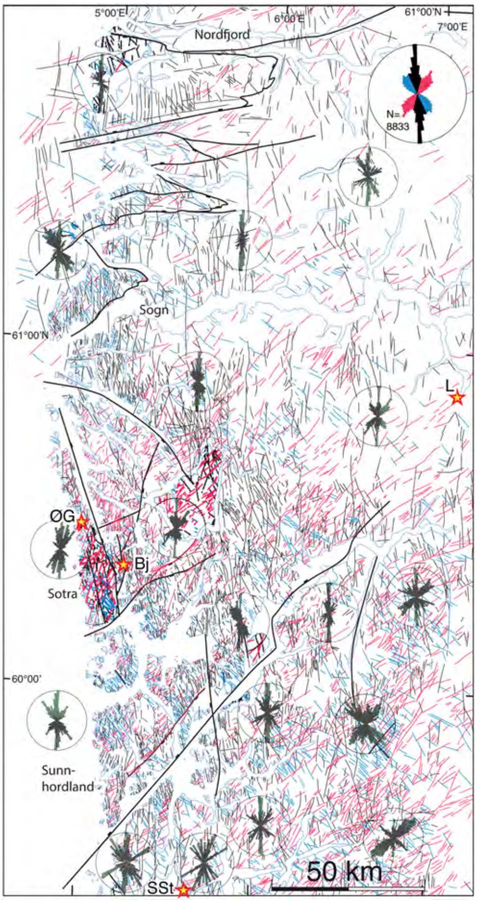

Fig. 6. Onshore fracture pattern from the interpretation of aerial photographs (8833 lineaments) supplied by field observations. Larger faults are indicated with thicker black lines. Rose diagrams are presented for subareas and for the total dataset. Rose diagram and lineaments are colour-coded according to trend (see online version for colours).

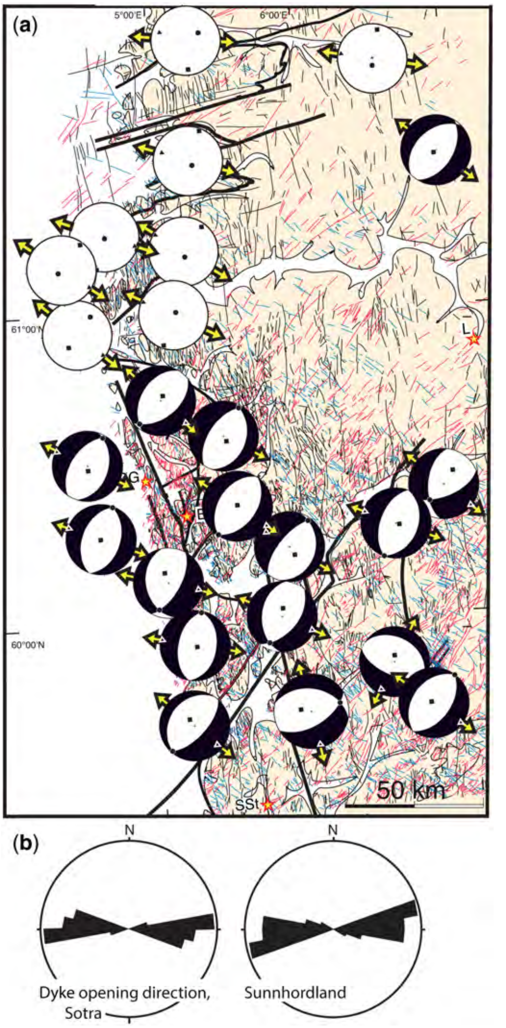

Fig. 7. (**a**) Kinematics from fault-slip analysis of fault populations from locations covered by the plots. Arrows represent the extension direction, which is mostly NW–SE. 'Beachballs' show fields of shortening (black), extension (white) and principal axes. Northern observations from Séranne & Séguret (1987) and Chauvet & Séranne (1994). (**b**) Opening directions (east–west) as determined from Permo-Triassic dykes in Sotra and Sunhordland (Fig. 6).

Field observations suggest that many of the onshore brittle structures interpreted in Figure 6 are steep, although low-angle structures also exist. The vast majority of these structures range from the NW to the NE. A strong coast-parallel (north–south) set is generally present (see also Fig. 4), together with a NW- and a NE-trending population. In addition, a series of more east–west-striking faults occur in the area associated with the Devonian basins (Fig. 4).

NE-trending faults overprinted by coast-parallel faults

The occurrence of at least three different strike populations suggests that the brittle faults and fractures shown in Figure 6 did not form in a single stress field. Kinematic fault-slip analysis indicates a strong influence of NW–SE stretching, as portrayed in Figure 7, and field work has shown that striated NE–SW-trending faults, commonly associated with epidote mineralization, are particularly well represented among the faults associated with NW–SE

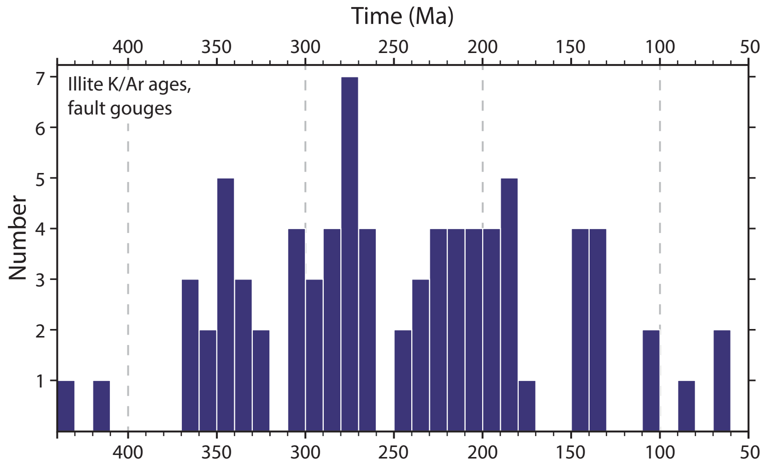

Fig. 8. Histogram of K–Ar illite ages from 25 sampled faults in West Norway. Three grain-size fractions (2–6, <2 and <0.2 μm) were dated for each sample. Note that some faults show evidence of repeated reactivation and, therefore, some ages are mixed. However, as a first-order interpretation, main periods of fault activity occurred in the Early Carboniferous, Permian, Triassic–Early Jurassic and latest Jurassic–earliest Cretaceous. Ages from Ksienzyk (2012), Arsenijevic (2013) and Woznitza (2014).

extension. This is also the extension direction portrayed by ductile (Mode I and II) Devonian extensional fabrics and structures, and it has been suggested that the population of brittle faults consistent with NW–SE extension represents the brittle continuation of Devonian ductile extension, and that they may have started to generate when the currently exposed level of the crust crossed the plastic–brittle transition (Fossen 2000). This assumption is consistent with approximately 395 Ma U–Pb dates of sphene on some of these early onshore fractures west of Bergen (Larsen *et al.* 2003).

Field observations show that NE–SW-trending faults are transected by north–south-trending faults and fractures, some of which are associated with dykes of Permo-Triassic age (Færseth *et al.* 1976; Torsvik *et al.* 1997; Fossen & Dunlap 1999) (Fig. 2). The kinematics of these dykes, as revealed by steps and jogs, consistently indicate east–west opening (Fig. 7), in concert with the Permo-Triassic rift-related faulting in the North Sea. Hence, in simple terms, there seems to have been a change from NW–SE Devonian to east–west Permo-Triassic extension.

Illite K–Ar fault gouge dating

An ongoing fault-dating project employs dating of authigenic illite from fault gouge found in exposed faults in West Norway by means of the K–Ar method (Ksienzyk 2012; Ksienzyk *et al.* 2012; Arsenijevic 2013; Woznitza 2014). A summary of ages from 25 faults from the onshore area is shown in Figure 8. For each sample, three grain-size fractions of 2–6, <2 and <0.2 μm were analysed.

Illite grows in active faults due to the combined effects of grain comminution caused by the crushing of the host rock and alteration by circulating fluids, thus providing a geochronometer with the potential to date fault activity (e.g. Solum *et al.* 2005; Tagami 2012). When a range of grain-size fractions are analysed, many faults yield dispersed ages that are correlated with grain size. In sedimentary rocks, this is commonly interpreted as a mixing of coarse-grained, older detrital illite from the host rock with fine-grained, younger authigenic illite from the fault (van der Pluijm *et al.* 2001; Solum *et al.* 2005). Crystalline rocks, like the basement of West Norway, are originally devoid of clay minerals, so that a potential contamination with detrital illite from the host rock is not an issue, and all illite ages should correspond to neocrystallization of illite in the fault. Nevertheless, many faults in crystalline rocks also show dispersed ages that are correlated with grain size. This age dispersion can be explained either by contamination of the coarser fractions with other K-bearing minerals from the host rock or by fault reactivation resulting in several generations of authigenic illite (Zwingmann & Mancktelow 2004; Zwingmann *et al.* 2010; Davids *et al.* 2013; Bense *et al.* 2014; Torgersen *et al.* 2014, 2015).

While contamination with K-bearing minerals from the host rock might be a contributing factor in some of the samples, we interpret most of the age dispersion in the dataset presented in Figure 8 to be caused by fault reactivation. Consequently, the oldest illite ages provide a minimum age of fault formation, while younger ages are generally interpreted as episodes of fault reactivation. With this in mind, main periods of fault activity could be identified in the Early Carboniferous, Permian, Triassic–Early Jurassic and around the Jurassic–Cretaceous boundary. The latter two periods correlate roughly with the two phases of North Sea rifting, and pulses of dyke intrusion at around 250 and 220 Ma. However, it is interesting that fault gouges with a significant clay content seem to have already developed in the Late Devonian, and that marked onshore brittle faulting occurred prior to the onset of North Sea rifting. The dataset includes faults with both NW–SE, north–south and NE–SW orientations, many of them with a pre-Triassic age component (Ksienzyk 2012) (Fig. 8), suggesting that a range of fault orientations were established at the onset of, or in the early stages of, North Sea rifting, with evidence of repeated reactivation showing that similar offshore basement faults may have influenced the fault pattern observed in the rift basin-fill. The long history of activity seen in many faults, with often multiple episodes of reactivation, is demonstrated by two examples, including the Lærdal samples referred to above. The other locality is at Skjoldastraumen; both localities are shown in Figure 2.

The Skjoldastraumen sample (SSt in Fig. 2) comes from a minor fault along one of several pronounced coast-parallel faults that host Permian and Triassic dykes. Illites from this sample yielded a middle Carboniferous (320 ± 9 Ma) K–Ar age for the coarsest fraction (2σ analytical errors), and middle Permian (274 ± 6 Ma) and Late Triassic (227 ± 7 Ma) ages for the intermediate and finest fractions, respectively. The fact that illite grew as early as in the Carboniferous suggests that at least some elements of these NNW-trending coast-parallel fractures were established prior to dyke intrusion and Permo-Triassic rifting. The increasingly younger ages in the smaller grain-size fractions indicate renewed fault activity in the Late Triassic, most probably contemporaneous with Triassic (*c.* 220 Ma) dyke intrusion recorded along these lineaments (Fossen & Dunlap 1999).

A sample (BG-129a) from the NE-trending Lærdal–Gjende Fault (locality L in Fig. 2) (Fig. 9) yielded latest Jurassic–earliest Cretaceous ages (149 ± 4 and 144 ± 2 Ma, respectively) for the two coarser grain-size fractions. The finest fraction yielded a younger age (64 ± 1 Ma), suggesting a Paleocene reactivation of the fault. A second sample (BG-129b) yielded an Early Jurassic age (191 ± 3 Ma) for the coarsest fraction. However, this grain-size fraction contained considerable amounts of K-feldspar and the age does not, therefore, reflect the timing of illite crystallization, but, rather, should be considered as a mixed illite/inherited K-feldspar age. The intermediate grain-size fraction, with only trace amounts of K-feldspar, gave an Early Cretaceous age (142 ± 2 Ma) that is almost identical to the latest Jurassic–earliest Cretaceous ages of BG-129a. The finest fraction, with an age of 106 ± 2 Ma, again suggests a later (Late Cretaceous or younger) reactivation. The results thus show the main phase of illite growth at around 150–140 Ma, corresponding to the younger

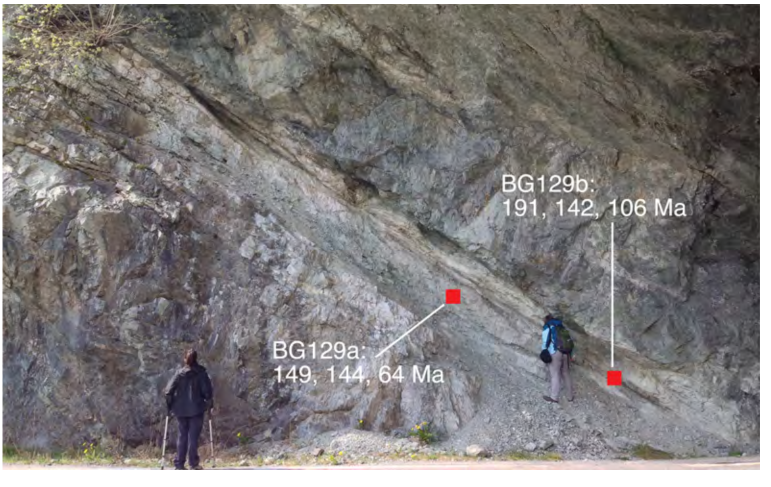

Fig. 9. Road section through the Lærdal–Gjende Fault gouge at the Lærdal locality (Fig. 2), showing sample locations for K–Ar illite dating. The main period of illite growth is latest Jurassic–earliest Cretaceous with evidence of a later Albian–Palaeogene reactivation.

palaeomagnetic age found by Andersen *et al.* (1999). This is in agreement with the fact that we sampled the non-cohesive part of the fault, which is considered to be the most recently active part of the fault. Hence, there is strong evidence for brittle reactivation of the low-angle Lærdal–Gjende Fault at the time of rifting in the North Sea and the Oslo Rift. Oblique and horizontal striations on slip surfaces along the Lærdal–Gjende Fault are seen in the field, which, given its oblique orientation to the Permo-Triassic extension direction recorded by dykes along the coast, fit with oblique reactivation at the same time as east–west extension during North Sea rifting.

$^{40}Ar/^{39}Ar$ *dating of feldspar*

Some of the faults and fractures in the felsic basement gneisses in West Norway show evidence of K-feldspar alteration in a centimetre-wide pink alteration rim around the faults and fractures (Fig. 10e). Close examination of such an example from

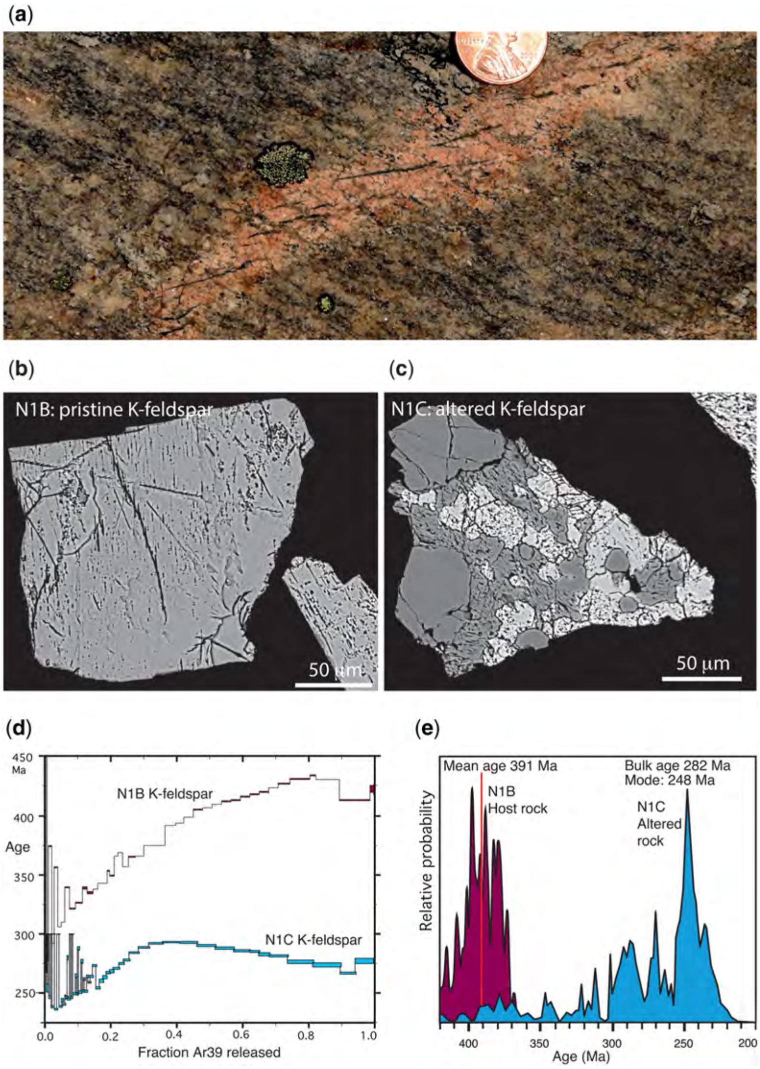

Fig. 10. (**a**) Alteration of K-feldspar around fractures in Proterozoic gneiss, Øygarden Complex west of Bergen. (**b**)–(**c**) SEM images of unaltered (from sample N1B) and altered (from sample N1C) feldspar grains from within and outside of an alteration rim, respectively. N1B feldspar is altered into epidote minerals, quartz and new K-feldspar. (**d**) $^{40}Ar/^{39}Ar$ age spectra for the two samples. (**e**) $^{40}Ar/^{39}Ar$ age probability density plot for the two samples, showing a significant younger age peak (*c.* 250 Ma) for the altered feldspar. See the text for the discussion.

the Øygarden Complex west of Bergen (starred locality ØG in Fig. 2) shows that the original cryptoperthitic K-feldspar is altered into a mixture of new K-feldspar, epidote, quartz and iron oxides. We sampled altered K-feldspar from within the alteration rim (N1C) and pristine feldspar from the alteration rims (N1B) from the host rock several metres away (Fig. 10a, b).

A $^{40}Ar/^{39}Ar$ age spectrum for a detailed step-heating experiment of the N1B K-feldspar and the associated multidomain solution were presented by Dunlap & Fossen (1998). The spectrum (N1B in Fig. 10c) is consistent with simple volume diffusion theory, which predicts that age spectra should increase monotonically with progressive ^{39}Ar release because natural ^{40}Ar concentrations would be higher in more retentive sites (Lovera *et al.* 2002). Hence, we interpret the data to reflect closure of cryptoperthite to diffusive argon loss as it cooled through the temperature range from approximately 320 to 180°C.

The altered K-feldspar N1C (Fig. 10b) yields a very different age spectrum that shows an intermediate age maximum at around 40% of ^{39}Ar released (Fig. 10c), and with a bulk age of 282 Ma and a peak age in the probability density plot at approximately 250 Ma (i.e. significantly lower than for the pristine N1C feldspar) (Fig. 10d). Lovera *et al.* (2002) found, based on an extensive database, that intermediate-age maxima tend to be yielded by K-feldspars that have been deformed in shallow, high-strain environments adjacent to brittle faults. Hence, our data and observations can be interpreted in the framework of strong alteration of the K-feldspar in the fault zone around 240 Ma. As for illite dates, the age is related to alteration caused by the circulation of fluids rather than directly dating fault activity. Hence, the age represents a minimum age of formation for faults and fractures with alteration haloes in the basement west of Bergen. The approximate 250 Ma age of alteration corresponds well with Permo-Triassic dyke intrusion (260–250 and 230–220 Ma) and early rifting in the adjacent North Sea Rift. It is also worth noting that Steltenpohl *et al.* (2011) analysed similar red-coloured K-feldspar from the Hadselfjorden Fault Zone in Lofoten in North Norway, obtaining a $^{40}Ar/^{39}Ar$ age spectrum that showed apparent ages of between 207 and 239 Ma, which they interpreted as the initiation of that fault zone in the Late Triassic.

The North Sea Rift

The northern North Sea Rift is mainly the product of a Permo-Triassic rift phase followed by a second phase that initiated during deposition of the Middle Jurassic Brent Group and locally affected Early Cretaceous strata (e.g. Badley *et al.* 1988; Roberts *et al.* 1995; Færseth 1996; Christiansson *et al.* 2000; Bell *et al.* 2014). In the Permian basin south of the Hardangerfjord Shear Zone, there is evidence of rifted Carboniferous and older sedimentary and volcanic rocks underneath Middle–Late Permian Zechstein salt (e.g. Martin *et al.* 2002; Heeremans & Faleide 2004), consistent with Early Permian rifting simultaneous with the main period of faulting in the Oslo Rift (the Oslo Rift initiated in the Late Carboniferous and terminated in the Early Triassic, according to Larsen *et al.* 2008).

Basement wells north of the Hardangerfjord Shear Zone have been drilled on structural highs, directly from Jurassic or Triassic sediments into metamorphic basement with no evidence of Permian or Carboniferous strata. A key well on the Horda Platform in this respect is well 31/6-1 (Fig. 11), where lower Triassic beds rest on basement that is seen, from cores, to consist of alternating granitic and amphibolitic gneiss. However, this well, like all other basement wells in the northern North Sea, was drilled at the high crest of a fault block. Down-flank from the well there is an undrilled lower part of a wedge-shaped sequence of strata older than the lower Triassic encountered in the well. Hence, these strata may be of earliest Triassic or Upper Palaeozoic age, opening the possibility that rifting was already going on in the Permian, probably in concert with (?Early) Permian rifting in the southern North Sea and the Oslo Rift. In addition, some near-top-basement reflective packages probably represent layered Caledonian allochthonous units (Fig. 11). Early Triassic synrift sequences on the Horda Platform were overlain by a Middle Triassic–Middle Jurassic post-rift package, followed by Phase 2 rifting with a relatively thin late-Jurassic synrift sequence and a thick Cretaceous–Cenozoic post-rift sequence (Badley *et al.* 1988; Roberts *et al.* 1995).

One of the assumptions commonly made is that, at the onset of rifting, the extremely overthickened Caledonian crust had returned to normal thickness. Several authors (e.g. Færseth 1996; Odinsen *et al.* 2000) have assumed that the Permian crustal thickness is represented by the current crustal thickness in the onshore are, which is around 32 km near the coast. Such an assumption does not consider the effect of post-Early Permian exhumation, which can now be quantified based on recent thermochronological data, as compiled in Figure 12. This compilation suggests that rocks currently exposed along the coast were close to or slightly above 200°C in the Early Permian, corresponding to a depth of approximately 8 km and, hence, an Early Permian crustal thickness of approximately 40 km. This is the current thickness closer to the Caledonian

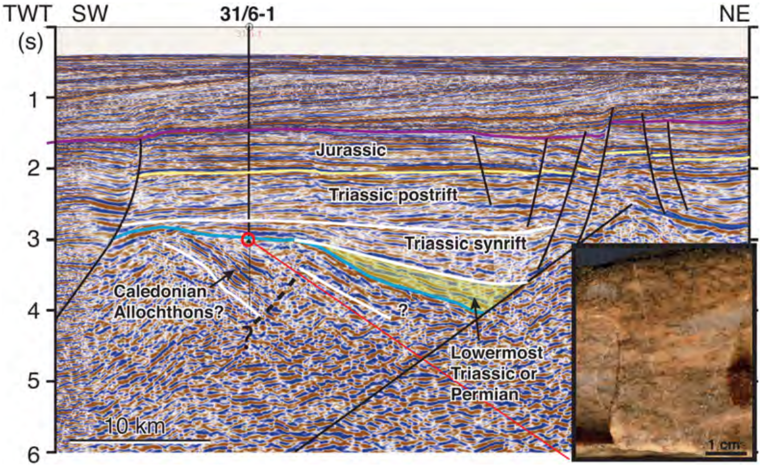

Fig. 11. Seismic section through well 31/6-1 with a picture of the basement (Caledonian) from the core. The lower part of the half-graben wedge to the east of the well is not drilled, but is likely to consist of earliest Triassic or Permian sedimentary layers. For the location, see Figure 2.

foreland (excluding the Oslo Rift) (Ebbing *et al.* 2012) and a more likely estimate of the crustal thickness as rifting initiated. The fact that the Caledonian crust was reduced to normal thickness by the Early Permian allows for an important distinction between Devonian extension, which represents tectonic

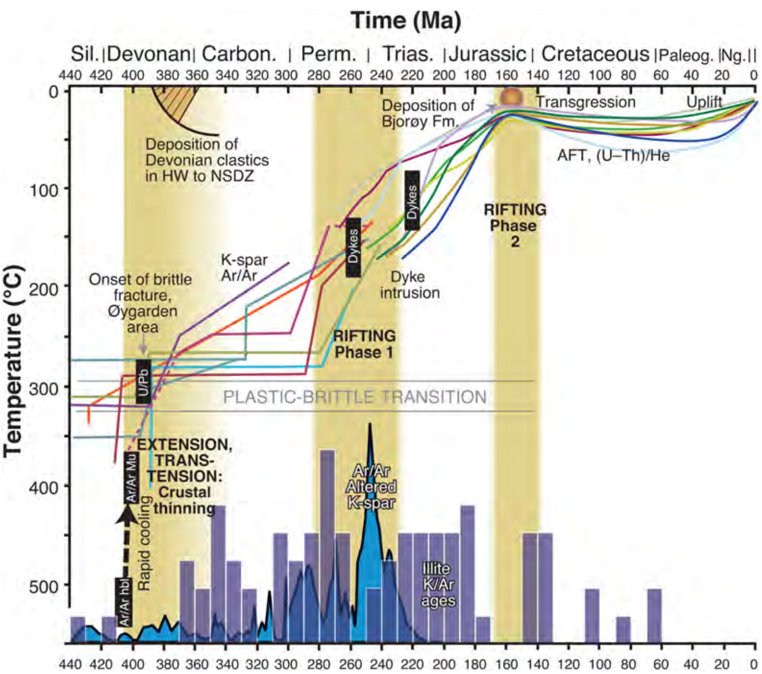

Fig. 12. Temperature–time graph from the onshore area around Bergen, based on geochronological data. The U–Pb age is from Larsen *et al.* (2003), Ar/Ar data and K-feldspar models from Dunlap & Fossen (1998), dyke ages from Færseth *et al.* (1976) and Fossen & Dunlap (1999), and the AFT and (U–Th)/He models from Ksienzyk *et al.* (2014). The bottom Ar/Ar age spectrum is from Figure 10e, while the K–Ar histogram is from Figure 8. AFT, apatite fission track.

thinning of overthickened Caledonian crust, and the two-phased North Sea rifting that thinned a crust of normal thickness.

Relationships between onshore and offshore structures

An interpretation of top basement across the northern North Sea Rift is shown in Figure 2, together with major faults, most of which are basement-rooted. 'Basement' is here loosely defined as anything older than mid Permian, including sub-Zechstein Palaeozoic packages observed on the Sele High and Devonian–Carboniferous strata on the East Shetland Platform (Platt 1995; Marshall & Hewett 2003). The interpretation, which is based on a large number of 2D and 3D seismic data and basement wells, is somewhat uncertain, particularly in the deeper parts such as the Viking Graben, but gives a qualitative picture of the effect that the two rift phases had on the early Permian surface.

Most of the first-order basement structures, such as the Utsira High, Stord Basin and Viking Graben, are confirmed by gravity and magnetic maps (Fig. 13). Along the coast, several of the allochthonous units in the hanging wall to the Nordfjord–Sogn Detachment Zone, Bergen Arcs Shear Zone and Karmøy Shear Zone are associated with high positive gravity anomalies. Similar anomalies over several of the offshore basement highs indicate that these allochthons also occur in significant amounts in the northern North Sea, as confirmed locally by basement wells: for instance, on the Utsira High (Slagstad *et al.* 2011). Similarly, negative gravity and magnetic anomalies mark the wide basins in the hanging wall to the Øygarden Fault System, particularly the Stord Basin, as major negative structures. Also, the onshore Devonian Hornelen Basin shows a marked negative magnetic anomaly, suggesting the possibility that Devonian basins may contribute to negative anomalies offshore, notably in the Stord Basin and parts of the North Viking Graben and East Shetland Platform.

The major faults on the east side of the Viking Graben, such as the Øygarden Fault System, are Permo-Triassic in origin (Steel 1993; Bell *et al.* 2014). Permo-Triassic faults in the northern North Sea Rift have generally been described as having an overall north–south orientation (Færseth 1996), but it is clear from new data that many of the larger Permo-Triassic faults have more curved and segmented shapes than those presented in earlier works. For example, the Øygarden Fault System consists of two large and one small segment, all of which curve considerably in map view (Fig. 2). Another example is the linked fault system along the east side of the Utsira High, which is also the largest fault in the Horda Platform/Stord Basin area. This fault system, which generated the deepest portion of the Stord Basin, displays curved segments, of which the northern segment curves to the NE towards the Øygarden Fault System. Together with the southern segment of the Øygarden Fault System, this fault defines the Stord Basin as a relatively isolated basin in the North Sea.

Regarding the relationship between these major Permo-Triassic faults and Devonian extension structures, we find that some of the major rift faults form on top of packages of dipping reflections that we interpret as Devonian Mode II extensional shear zones, whereas many others, such as the Øygarden Fault System and its northern extension, bear no sign of being formed by reactivation of pre-existing structures, and cut through low-angle Devonian fabrics and detachments. The offshore extensions of the Karmøy Shear Zone and Hardangerfjord Shear Zone are outstanding examples of the former, where Devonian basement shear zones influence rift-related brittle faulting. In detail, the Permo-Triassic faults are steeper in their upper parts, but apparently merge with the shear zones at depth (Fig. 14a, b). There is evidence from seismic mapping below the fjord SE of Karmøy that the Karmøy Shear Zone reactivated as a brittle fault to form a Mesozoic half-graben (Bøe *et al.* 2010), and, as discussed earlier, there is geochronological evidence for onshore brittle reactivation of the Hardangerfjord Shear Zone/Lærdal-Gjende Fault in the Permian and Late Jurassic–Early Cretaceous. The curved fault defining the east margin of the Utsira High is another example, where the underlying package of reflectors is interpreted as a shear zone that is likely to represent an east- to SE-dipping Devonian Mode II shear zone (the Utsira Shear Zone in Fig. 2) (Fig. 14c), representing a change in polarity of the system of Devonian extensional shear zones across the Horda Platform.

Domain boundaries

The Hardangerfjord Shear Zone and Karmøy Shear Zone appear to have a marked influence on the fault pattern in the Horda Platform, as they are marked by several NE–SW-trending faults at top basement (Fig. 2) and higher levels. These are two (1 and 2 in Fig. 2) of several somewhat diffuse structural boundaries that subdivide the rift into distinct structural domains, each of which have their own characteristic fault pattern and/or fault polarity. The next one to the north is represented by the northern part of the Utsira Shear Zone and its extension to the NE (Boundary 3 in Fig. 2), which marks a boundary across which the Øygarden Fault System abruptly changes from west to east dipping, and where a horst appears on the north side. This

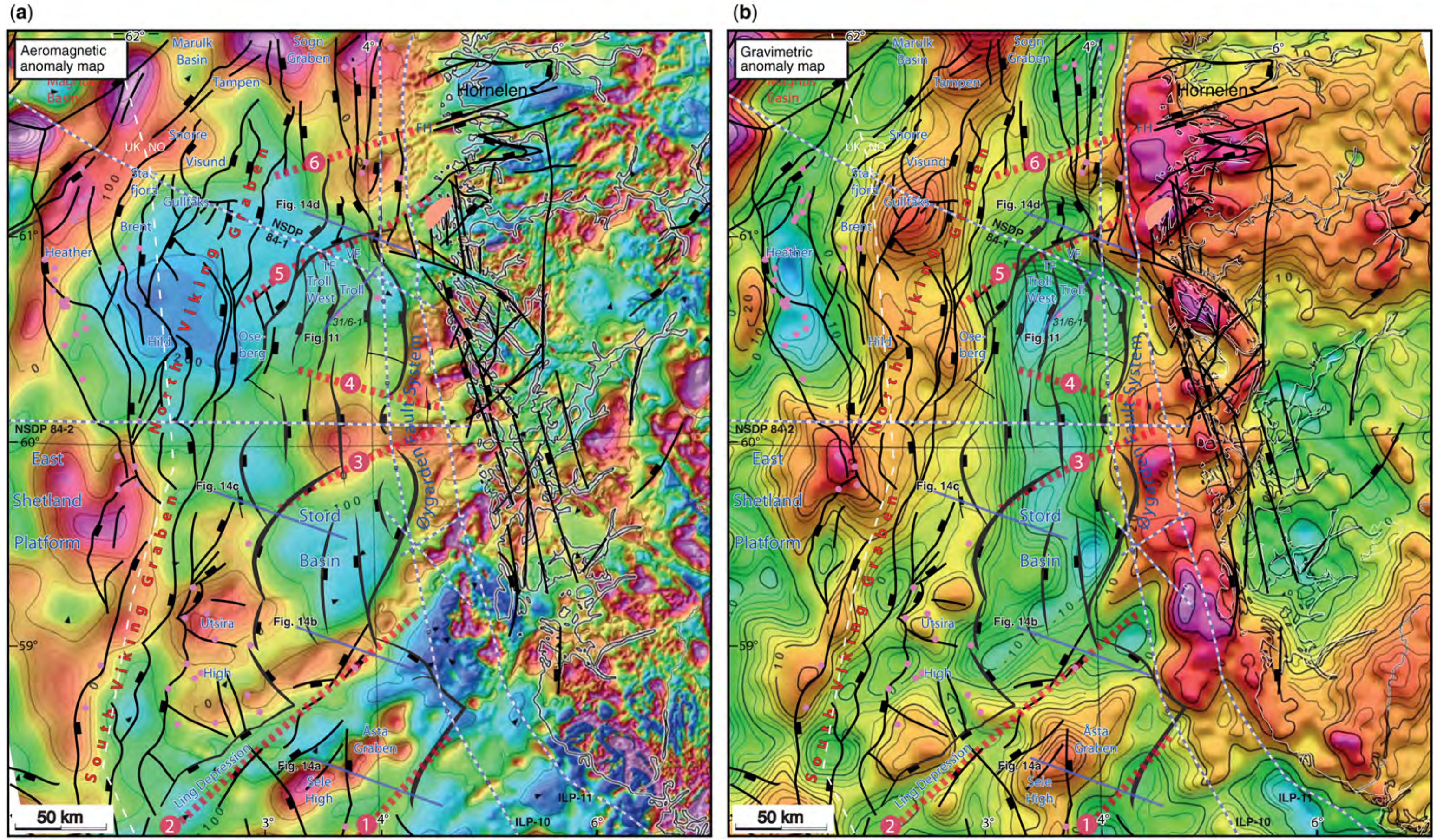

Fig. 13. (**a**) Aeromagnetic and (**b**) gravity map of the area covered by Figure 2. Warm colours indicate positive anomalies, whereas cold colours reflect negative anomalies. From Olesen *et al.* (2010*a*, *b*). Faults from Figure 2.

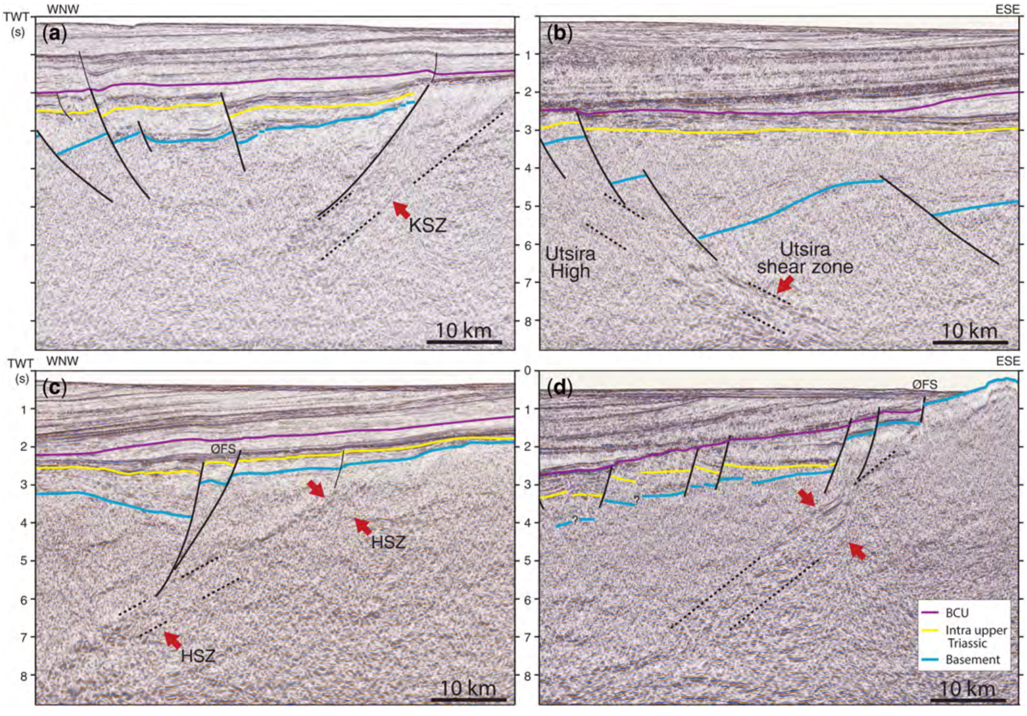

Fig. 14. Four seismic images across zones of basement reflections interpreted as Devonian Mode II extension shear zones. Top basement is top crystalline basement in these sections, but the interpretation is uncertain in the deeper parts. Preliminary depth conversions suggest that the shear zones are dipping at 20–30° (apparent dips). See Figure 2 for the location. BCU, Base Cretaceous Unconformity.

horst disappears to the north across Boundary 4 as the Øygarden Fault System flips back to become west dipping. There is also a difference in Jurassic strain from very low in the Stord Basin to moderately high in the Troll–Oseberg area, accommodated by strain transfer along Boundary 3. Boundaries 3 and 4 project onshore to the place where the Sunhordland Detachment and the Totland Fault (SD and ToF in Fig. 2) separate the Proterozoic basement west of Bergen from the allochthonous units to the south, although their relationship with these structures is unclear.

Another boundary (Boundary 5) is found at 61°N, north of the Troll and Oseberg fields (Fig. 2). Here, the west-dipping Øygarden Fault System, Vette Fault and Tusse Fault (VF and TF in Fig. 2) terminate or make remarkable steps (Badley *et al.* 1988; Barling 2014) across the NNE-trending structure. For this structure, which was also noted by Færseth *et al.* (1995) and Færseth (1996) as a domain-bounding structure, we recognize a relatively shallowly dipping set of reflectors (Fig. 14d) that most probably represents a NW-dipping basement shear zone that extends from near the surface down to the reflective lower crust at around 8 s two-way time (TWT) (approximately 16 km). The location and orientation of this structure suggest that it may be connected to the Dalsfjord Fault (Fig. 4), which is interpreted as a Devonian fault that was reactivated in the Permian and latest Jurassic–earliest Cretaceous (Eide *et al.* 1997). A set of south(east)-dipping reflections also occur on the deep seismic line ILP10 in this area (just north of 59° in Fig. 3). The gravity and magnetic anomaly maps (Fig. 13) give some support to this interpretation, which seems more likely than the one presented by Færseth *et al.* (1995), where the Nordfjord–Sogn Detachment Zone was abruptly bent westwards into the North Sea to connect with this domain boundary.

About 50–60 km to the north, we suggest a possible connection between the onshore Florø Horst (Figs 2 & 4) and the change in offshore fault arrangement in its offshore extension (6 in Fig. 2). This diffuse structure marks the southern termination of the Sogn Graben, which at this point steps westwards to the North Viking Graben. In this case, there are clear magnetic and gravimetric lineaments extending the Florø Horst offshore towards Boundary 6.

Concluding remarks

The Baltica–Laurentia continent–continent collision produced a highly anisotropic crust in the northern North Sea region and its margins that was prone to reactivation at the onset of post-collisional extension shortly prior to 400 Ma. The reactivation of the basal thrust or décollement zone confirms that reactivation of very-low-angle (*c.* 5°) shear zones is possible, provided that the zone is sufficiently weak. Most of the secondary (Mode II) extensional shear zones and faults of Devonian age are steeper, but several are still low angle, and the detachment underlying the Devonian Hornelen Basin must have been very low angle. We have presented new geochronological data that confirm that Mode II structures reactivated as post-Devonian brittle faults, several of them as low-angle faults (7° for the Hornelen Detachment and *c.* 25° for the Lærdal–Gjende Fault), giving additional evidence in favour of post-Devonian reactivation of low-angle normal faults. Interestingly, several of the pre-rift shear zones and faults reactivated in spite of being unfavourably orientated for slip (highly oblique to the extension direction), suggesting that they were mechanically weak structures at the time of North Sea rifting.

Even though the large Mode II shear zones reactivated during rifting, a large array of steeper brittle faults formed, both onshore (some with Permo-Triassic dykes along them) and offshore, where some of them accumulated kilometre-scale offsets. Isotope data presented in this work suggest a long history of brittle clay-gouge forming faulting that can be dated back to the Late Devonian, perhaps even for coast-parallel faults that parallel Permo-Triassic faults of the Horda Platform to the west. Hence, it is possible that they had some influence on the locations and orientations of the Permo-Triassic rift-faults. The wide range of illite K–Ar ages together with K-feldspar Ar/Ar ages shows that the fault network on the onshore rift shoulder was active before, during, as well as after the period of North Sea rifting. The entrapment and deformation of Late Jurassic sediments in a coast-parallel fault zone west of Bergen supports this scenario (Fossen *et al.* 1997).

We suggest, based on the seismic examples presented in this work, that even if the more-or-less north–south-trending faults accumulated most of the strain in the rift, large-scale Devonian Mode II shear zones were also reactivated offshore during both phases of North Sea rifting. Prime examples are the Hardangerfjord and Karmøy shear zones, and we propose the existence of a similar but oppositely dipping Devonian shear zone along the east flank of the Utsira High, here named the Utsira Shear Zone. These Devonian Mode II shear zones influenced the fault-block configuration of the northern North Sea Rift by creating a series of domain boundaries. The rift-related faults form uniform arrays between the boundaries, but lose offset, terminate or bend as they approach these segment boundaries. We may speculate that the southern termination of the Sogn Graben is related to the presence of Boundary 6 (the offshore extension of the Florø Horst), creating a right-lateral step to the North Viking Graben as the faults were arrested at this boundary. Furthermore, the possibility that the other steps portrayed by the Viking Graben may be related to pre-existing structures originating in the basement should not be ruled out.

A similar influence of oblique pre-rift basement structures on rift geometry has been postulated elsewhere: for instance, in the East African Rift (Morley *et al.* 2004), the Suez Rift (Bosworth 2015) and the Brazilian Tucano Basin (Milani & Davison 1988). The Scandinavian Caledonides are special by their high content of pre-rift extension structures that probably have a larger influence on the North Sea rifting than Caledonian thrusts. The fact that fundamental Devonian extension structures are much better developed in the Norwegian Caledonides than in the Scottish Caledonides could potentially have influenced the location of the rift, particularly the Permo-Triassic basin formation on the Horda Platform. In order to explore such questions in more depth, there is a need to continue the mapping of basement structures in the North Sea Rift.

This work was supported by the MultiRift Petromaks2 project 215591, financed by the Research Council of Norway and Statoil. Thanks to TGS for permission to publish the seismic examples, and to Chris Jackson, Rebecca Bell, Allan Roberts and an anonymous reviewer for making constructive comments on an earlier version of the manuscript.

References

Andersen, T.B. & Jamtveit, B. 1990. Uplift of deep crust during orogenic extensional collapse: a model based on field studies in the Sogn–Sunnfjord region of western Norway. *Tectonics*, **9**, 1097–1112.

Andersen, T.B., Torsvik, T.H., Eide, E.A., Osmundsen, P.T. & Faleide, J.I. 1999. Permian and Mesozoic extensional faulting within the Caledonides of central south Norway. *Journal of the Geological Society, London*, **156**, 1073–1080, http://doi.org/10.1144/gsjgs.156.6.1073

Arsenijevic, A.C. 2013. *Korngrößenabhängige Methoden zur Charakterisierung von Lettentonen: K–Ar-Datierung, Illit-Kristallinität und Illit-Polytypie*. BSc thesis, University of Göttingen.

Badley, M.E., Price, J.D., Dahl, C.R. & Agdestein, T. 1988. The structural evolution of the northern Viking Graben and its bearing upon extensional modes of basin formation. *Journal of the Geological Society,* *London*, **145**, 455–472, http://doi.org/10.1144/gsjgs.145.3.0455

Barling, T. 2014. *Growth of a major normal fault complex in the horda platform, North Sea*. MSc thesis, Imperial College.

Bassett, M.G. 2003. Sub-Devonian geology. *In*: Evans, D., Graham, C., Armour, A. & Bathurst, P. (eds) *The Millennium Atlas: Petroleum Geology of the Central and Northern North Sea*. Geological Society, London, 61–63.

Bell, R.E., Jackson, C.A.L., Whipp, P.S. & Clements, B. 2014. Strain migration during multiphase extension: observations from the northern North Sea. *Tectonics*, **33**, 1936–1963.

Bense, F.A., Wemmer, K., Löbens, S. & Siegesmund, S. 2014. Fault gouge analyses: K–Ar illite dating, clay mineralogy and tectonic significance – a study from the Sierras Pampeanas, Argentina. *International Journal of Earth Sciences*, **103**, 189–218.

Bøe, R., Fossen, H. & Smelror, M. 2010. Mesozoic sediments and structures onshore Norway and in the coastal zone. *Norges Geologiske Undersøkelse Bulletin*, **450**, 15–32.

Bosworth, W. 2015. Geological evolution of the Red Sea: historical background, review, and synthesis. *In*: Rasul, N.M.A. & Stewart, I.C.F. (eds) *The Red Sea*. Springer, Berlin, 45–78.

Braathen, A. 1999. Kinematics of post-Caledonian polyphase brittle faulting in the Sunnfjord region, western Norway. *Tectonophysics*, **302**, 99–121.

Brewer, M.S. & Smythe, D.K. 1984. MOIST and the continuity of crustal reflector geometry along the Caledonian–Appalachian orogen. *Journal of the Geological Society, London*, **141**, 105–120, http://doi.org/10.1144/gsjgs.141.1.0105

Butler, R.W.H. 2010. The Geological Structure of the North-West Highlands of Scotland - revisited: Peach et al. 100 years on. *In*: Law, R.D., Butler, R.W.H., Holdsworth, R.E., Krabbendam, M. & Strachan, R.A. (eds) *Continental Tectonics and Mountain Building: The Legacy of Peach and Horne*. Geological Society, London, Special Publications, **335**, 7–27, http://doi.org/10.1144/SP335.2

Chauvet, A. & M.& Séranne, 1994. Extension-parallel folding in the Scandinavian Caledonides: implications for late-orogenic processes. *Tectonophysics*, **238**, 31–54.

Christiansson, P., Faleide, J.I. & Berge, A.M. 2000. Crustal structure in the northern North Sea: an integrated geophysical study. *In*: Nøttvedt, A. *et al.* (eds) *Dynamics of the Norwegian Margin*. Geological Society, London, Special Publications, **167**, 15–40, http://doi.org/10.1144/GSL.SP.2000.167.01.02

Constenius, K.N. 1996. Late Paleogene extensional collapse of the Cordilleran foreland fold and thrust belt. *Geological Society of America Bulletin*, **108**, 20–39.

Davids, C., Wemmer, K., Zwingmann, H., Kohlmann, F., Jacobs, J. & Bergh, S.G. 2013. K–Ar illite and apatite fission track constraints on brittle faulting and the evolution of the northern Norwegian passive margin. *Tectonophysics*, **608**, 196–211.

Dobrzhinetskaya, L.F., Larsen, R.B., Sturt, B.A., Trønnes, R.G., Smith, D.C., Taylor, W.R. & Posukhova, T.V. 1995. Microdiamond in high-grade metamorphic rocks of the Western Gneiss region, Norway. *Geology*, **23**, 597–600.

Dunlap, W.J. & Fossen, H. 1998. Early Proterozoic orogenic collapse, tectonic stability, and late Paleozoic continental rifting revealed through thermochronology of K-feldspars, southern Norway. *Tectonics*, **17**, 604–620.

Ebbing, J., England, R.W., Korja, T., Lauritsen, T., Olesen, O., Stratford, W. & Weidle, C. 2012. Structure of the Scandes lithosphere from surface to depth. *Tectonophysics*, **536–537**, 1–24.

Eide, E., Torsvik, T.H. & Andersen, T.B. 1997. Absolute dating of brittle fault movements: late Permian and late Jurassic extensional fault breccias in western Norway. *Terra Nova*, **9**, 135–139.

Færseth, R.B. 1996. Interaction of Permo-Triassic and Jurassic extensional fault-blocks during the development of the northern North Sea. *Journal of the Geological Society, London*, **153**, 931–944, http://doi.org/10.1144/gsjgs.153.6.0931

Færseth, R.B., Macintyre, R.M. & Naterstad, J. 1976. Mesozoic alkaline dykes in the Sunnhordland region, western Norway: ages, geochemistry and regional significance. *Lithos*, **9**, 331–345.

Færseth, R.B., Gabrielsen, R.H. & Hurich, C.A. 1995. Influence of basement in structuring of the North Sea basin, offshore southwest Norway. *Norsk Geologisk Tidsskrift*, **75**, 105–119.

Fauconnier, J., Labrousse, L., Andersen, T.B., Beyssac, O., Duprat-Oualid, S. & Yamato, P. 2014. Thermal structure of a major crustal shear zone, the basal thrust in the Scandinavian Caledonides. *Earth and Planetary Science Letters*, **385**, 162–171.

Faulds, J.E. & Varga, R.J. 1998. The role of accommodation zones and transfer zones in the regional segmentation of extended terranes. *In*: Faulds, J.E. & Stewart, J.H. (eds) *Accommodation Zones and Transfer Zones: The Regional Segmentation of the Basin and Range Province*. Geological Society of America Special Papers, **323**, 1–45.

Fossen, H. 1992. The role of extensional tectonics in the Caledonides of South Norway. *Journal of Structural Geology*, **14**, 1033–1046.

Fossen, H. 2000. Extensional tectonics in the Caledonides: synorogenic or postorogenic?. *Tectonics*, **19**, 213–224.

Fossen, H. 2010. Extensional tectonics in the North Atlantic Caledonides: a regional view. *In*: Law, R.D., Butler, R.W.H., Krabbendam, M. & Strachan, R.A. (eds) *Continental Tectonics and Mountain Building: The Legacy of Peach and Horne*. Geological Society, London, Special Publications, **335**, 767–793, http://doi.org/10.1144/SP335.31

Fossen, H. & Dunlap, W.J. 1998. Timing and kinematics of Caledonian thrusting and extensional collapse, southern Norway: evidence from $^{40}Ar/^{39}Ar$ thermochronology. *Journal of Structural Geology*, **20**, 765–781.

Fossen, H. & Dunlap, W.J. 1999. On the age and tectonic significance of Permo-Triassic dikes in the Bergen-Sunnhordland region, southwestern Norway. *Norsk Geologisk Tidsskrift*, **79**, 169–178.

Fossen, H. & Hurich, C.A. 2005. The Hardangerfjord Shear Zone in SW Norway and the North Sea: a large-scale low-angle shear zone in the Caledonian crust.

Journal of the Geological Society, London, **162**, 675–687, http://doi.org/10.1144/0016-764904-136

Fossen, H., Mangerud, G., Hesthammer, J., Bugge, T. & Gabrielsen, R. 1997. The Bjorøy Formation: a newly discovered occurence of Jurassic sediments in the Bergen Arc System. *Norsk Geologisk Tidsskrift*, **77**, 269–287.

Freeman, B., Klemperer, S.L. & Hobbs, R.W. 1988. The deep structure of northern England and the Iapetus Suture zone from BIRPS deep seismic reflection profiles. *Journal of the Geological Society, London*, **145**, 727–740, http://doi.org/10.1144/gsjgs.145.5.0727

Gabrielsen, R.H., Fossen, H., Faleide, J.I. & Hurich, C.A. 2015. Mega-scale Moho relief and the structure of the lithosphere on the eastern flank of the Viking Graben, offshore southwestern Norway. *Tectonics*, **34**, 803–819, http://doi.org/10.1002/2014TC003778

Gee, D.G., Fossen, H., Henriksen, N. & Higgins, A.K. 2008. From the Early Paleozoic Platforms of Baltica and Laurentia to the Caledonide Orogen of Scandinavia and Greenland. *Episodes*, **31**, 44–51.

Gibbs, A.D. 1987. Deep seismic profiles in the northern North Sea. *In*: Brooks, J. & Glennie, K.W. (ed.) *Petroleum Geology of North West Europe*. Graham & Trotman, London, 1025–1028.

Hacker, B.R. 2007. Ascent of the ultrahigh-pressure Western Gneiss Region, Norway. *In*: Cloos, M., Carlson, W.D., Gilbert, M.C., Liou, J.G. & Sorensen, S.S. (eds) *Convergent Margin Terranes and Associated Regions: A Tribute to W.G. Ernst*. Geological Society of America Special Papers, **419**, 171–184.

Hacker, B.R., Andersen, T.B., Johnston, S., Kylander-Clark, A.R.C., Peterman, E.M., Walsh, E.O. & Young, D. 2010. High-temperature deformation during continental-margin subduction & exhumation: the ultrahigh-pressure Western Gneiss Region of Norway. *Tectonophysics*, **480**, 149–171.

Heeremans, M. & Faleide, J.I. 2004. Late Carboniferous–Permian tectonics and magmatic activity in the Skagerrak, Kattegat and the North Sea. *In*: Wilson, M., Neumann, E.-R., Davies, G.R., Timmermann, M.J., Heeremans, M. & Larsen, B.T. (eds) *Permo-Carboniferous Magmatism and Rifting in Europe*. Geological Society, London, Special Publications, **223**, 157–176, http://doi.org/10.1144/GSL.SP.2004.223.01.07

Henza, A.A., Withjack, M.O. & Schlische, R.W. 2011. How do the properties of a pre-existing normal-fault population influence fault development during a subsequent phase of extension? *Journal of Structural Geology*, **33**, 1312–1324.

Høeg, O.A. 1945. Contributions to the Devonian flora of western Norway III. *Norsk Geologisk Tidsskrift*, **25**, 183–192.

Hossack, J.R. 1984. The geometry of listric growth faults in the Devonian basins of Sunnfjord, W Norway. *Journal of the Geological Society, London*, **141**, 629–637, http://doi.org/10.1144/gsjgs.141.4.0629

Hossack, J.R. & Cooper, M.A. 1986. Collision tectonics in the Scandinavian Caledonides. *In*: Coward, M.P. & Ries, A.C. (eds) *Collision Tectonics*. Geological Society, London, Special Publications, **19**, 285–304, http://doi.org/10.1144/GSL.SP.1986.019.01.16

Hurich, C.A. & Kristoffersen, Y. 1988. Deep structure of the Caledonide orogen in southern Norway: new evidence from marine seismic reflection profiling. *Norges geologiske undersøkelse Special Publication*, **3**, 96–101.

Klemperer, S.L. & Matthews, D.H. 1987. Iapetus Suture located beneath the North Sea by BIRPS deep seismic reflection profiling. *Geology*, **15**, 195–198.

Krabbendam, M. & Dewey, J.F. 1998. Exhumation of UHP rocks by transtension in the Western Gneiss Region, Scandinavian Caledonides. *In*: Holdsworth, R.E., Strachan, R.A. & Dewey, J.F. (eds) *Continental Transpressional and Transtensional Tectonics*. Geological Society, London, Special Publications, **135**, 159–181, http://doi.org/10.1144/GSL.SP.1998.135.01.11

Ksienzyk, A.K. 2012. *From mountains to basins: Geochronological case studies from southwestern Norway, Western Australia and East Antarctica*. PhD thesis, University of Bergen.

Ksienzyk, A.K., Kohlmann, F., Dunkl, I., Wemmer, K., Jacobs, J. & Fossen, H. 2012. Late Caledonian orogenic collapse and Permian-Mesozoic rifting: dating onshore faults in SW Norway with low-temperature thermochronological methods. *Abstracts and Proceedings of the Geological Society of Norway*, **2**, 37.

Ksienzyk, A.K., Dunkl, I., Jacobs, J., Fossen, H. & Kohlmann, F. 2014. From orogen to passive margin: constraints from fission track and (U–Th)/He analyses on Mesozoic uplift and fault reactivation in SW Norway. *In*: Corfu, F., Gasser, D. & Chew, D.M. (eds) *New Perspectives on the Caledonides of Scandinavia and Related Areas*. Geological Society, London, Special Publications, **390**, 679–702, http://doi.org/10.1144/SP390.27

Larsen, B.T., Olaussen, S., Sundvoll, B.A. & Heeremans, M. 2008. The Permo-Carboniferous Oslo Rift through six stages and 65 million years. *Episodes*, **31**, 52–58.

Larsen, Ø., Fossen, H., Langeland, K. & Pedersen, R.B. 2003. Kinematics and timing of polyphase post-Caledonian deformation in the Bergen area, SW Norway. *Norwegian Journal of Geology*, **83**, 149–165.

Lovera, O.M., Grove, M. & Harrison, T.M. 2002. Systematic analysis of K-feldspar 40Ar/39Ar step heating results II: relevance of laboratory argon diffusion properties to nature. *Geochimica et Cosmochimica Acta*, **66**, 1237–1255.

Lutro, O. & Bryhni, I. 2000. *Bergrunnskart Florø 1118 III, M 1:50,000. Foreløpig utgave*. Norges geologiske undersøkelse, Trondheim.

Lutro, O. & Tveten, E. 1996. *Geologisk kart over Norge, berggrunnskart Årdal M 1:250,000*. Norges geologiske undersøkelse, Trondheim.

Marshall, J.E.A. & Hewett, A.J. 2003. Devonian. *In*: Evans, D., Graham, C., Armour, A. & Bathurst, P. (eds) *The Millennium Atlas: Petroleum Geology of the Central and Northern North Sea*. Geological Society, London, 65–81.

Martin, C.A.L., Stewart, S.A. & Doubleday, P.A. 2002. Upper Carboniferous and Lower Permian tectonostratigraphy on the southern margin of the Central North Sea. *Journal of the Geological Society, London*,

159, 731–749, http://doi.org/10.1144/0016-764900-174

Milani, E.J. & Davison, I. 1988. Basement control and transfer tectonics in the Recôncavo-Tucano-Jatobá rift, Northeast Brazil. *Tectonophysics*, **154**, 41–70.

Milnes, A.G., Wennberg, O.P., Skår, Ø., Koestler, A.G. 1997. Contraction, extension and timing in the South Norwegian Caledonides: the Sognefjord transect. *In*: Burg, J.-P. & Ford, M. (eds) *Orogeny Through Time*. Geological Society, London, Special Publications, **121**, 123–148, http://doi.org/10.1144/GSL.SP.1997.121.01.06

Morley, C.K., Nelson, R.A., Patton, T.L. & Munn, S.G. 1990. Transfer zones in the East African rift system and their relevance to hydrocarbon exploration in rifts. *American Association of Petroleum Geologists Bulletin*, **74**, 1234–1253.

Morley, C.K., Haranya, C., Phoosongsee, W., Pongwapee, S., Kornsawan, A. & Wonganan, N. 2004. Activation of rift oblique and rift parallel pre-existing fabrics during extension and their effect on deformation style: examples from the rifts of Thailand. *Journal of Structural Geology*, **26**, 1803–1829.

Norton, M. 1987. The Nordfjord-Sogn Detachment, W. Norway. *Norsk Geologisk Tidsskrift*, **67**, 93–106.

Nur, A., Ron, H. & Scotti, O. 1986. Fault mechanics and the kinematics of block rotations. *Geology*, **14**, 746–749.

Odinsen, T., Reemst, P., Beek, P.V.D., Faleide, J.I. & Gabrielsen, R.H. 2000. Permo-Triassic and Jurassic extension in the northern North Sea: results from tectonostratigraphic forward modelling. *In*: Nøttvedt, A. *et al.* (eds) *Dynamics of the Norwegian Margin*. Geological Society, London, Special Publications, **167**, 83–103, http://doi.org/10.1144/GSL.SP.2000.167.01.05

Olesen, O., Ebbing, J. *et al.* 2010*a*. *Gravity Anomaly Map, Norway and Adjacent Areas, Scale 1:3 Million*. Norges geologiske undersøkelse, Trondheim.

Olesen, O., Gellein, J. *et al.* 2010*b*. *Magnetic Anomaly Map, Norway and Adjacent Areas, Scale 1:3 Million*. Norges geologiske undersøkelse, Trondheim.

Osmundsen, P.T. & Andersen, T.B. 2001. The middle Devonian basins of western Norway: sedimentary response to large-scale transtensional tectonics? *Tectonophysics*, **332**, 51–68.

Platt, N.H. 1995. Structure and tectonics of the northern North Sea: new insights from deep penetration regional seismic data. *In*: Lambiase, J.J. (ed.) *Hydrocarbon Habitat in Rift Basins*. Geological Society, London, Special Publications, **80**, 103–113, http://doi.org/10.1144/GSL.SP.1995.080.01.05

Roberts, A.M., Yielding, G., Kusznir, N.J., Walker, I.M. & Dorn-Lopez, D. 1995. Quantitative analysis of Triassic extension in the northern Viking Graben. *Journal of the Geological Society, London*, **152**, 15–26, http://doi.org/10.1144/gsjgs.152.1.0015

Rosendahl, B.R., Reynolds, D.J. *et al.* 1986. Structural expressions of rifting: lessons from Lake Tanganyika, Africa. *In*: Frostick, L.E., Renaut, R.W., Reid, I. & Tiercelin, J.J. (eds) *Sedimentation in the African Rifts*. Geological Society, London, Special Publications, **25**, 29–43, http://doi.org/10.1144/GSL.SP.1986.025.01.04

Séranne, M. & Séguret, M. 1987. The Devonian basins of western Norway: tectonics and kinematics of an extending crust. *In*: Coward, M.P., Dewey, J.F. & Hancock, P.L. (eds) *Continental Extensional Tectonics*. Geological Society, London, Special Publications, **28**, 537–548, http://doi.org/10.1144/GSL.SP.1987.028.01.35

Slagstad, T., Davidsen, B. & Daly, J.S. 2011. Age and composition of crystalline basement rocks on the Norwegian continental margin: offshore extension and continuity of the Caledonian–Appalachian orogenic belt. *Journal of the Geological Society, London*, **168**, 1167–1185, http://doi.org/10.1144/0016-76492010-136

Smith, D.C. & Lappin, M.A. 1989. Coesite in the Straumen kyanite-eclogite pod, Norway. *Terra Nova*, **1**, 47–56.

Solum, J.G., van der Pluijm, B.A. & Peacor, D.R. 2005. Neocrystallization, fabrics and age of clay minerals from an exposure oft he Moab Fault, Utah. *Journal of Structural Geology*, **27**, 1563–1576.

Steel, R. 1993. Triassic–Jurassic megasequence stratigraphy in the Northern North Sea: rift to post-rift evolution. *In*: Parker, J.R. (ed.) *Petroleum Geology of Northwest Europe: Proceedings of the 4th Conference*. Geological Society, London, 299–315, http://doi.org/10.1144/0040299

Steel, R., Siedlecka, A. & Roberts, D. 1985. The Old Red Sandstone basins of Norway and their deformation: a review. *In*: Gee, D.G. & Sturt, B.A. (eds) *The Caledonide Orogen – Scandinavia and Related Areas*. John Wiley & Sons, Chichester, 293–315.

Steltenpohl, M.G., Moecher, D., Andresen, A., Ball, J., Mager, S. & Hames, W.E. 2011. The Eidsfjord shear zone, Lofoten–Vesterålen, north Norway: an Early Devonian, paleoseismogenic low-angle normal fault. *Journal of Structural Geology*, **33**, 1023–1043.

Tagami, T. 2012. Thermochronological investigation of fault zones. *Tectonophysics*, **538–540**, 67–85.

Torgersen, E., Viola, G., Zwingmann, H. & Harris, C. 2014. Structural and temporal evolution of a reactivated brittle-ductile fault – Part II: timing of fault initiation and reactivation by K–Ar dating of synkinematic illite/muscovite. *Earth and Planetary Science Letters*, **407**, 221–233.

Torgersen, E., Viola, G., Zwingmann, H. & Henderson, I.H.C. 2015. Inclined K–Ar illite age spectra in brittle fault gouges: effects of fault reactivation and wall-rock contamination. *Terra Nova*, **27**, 106–113.

Torsvik, T.H., Andersen, T.B., Eide, E.A. & Walderhaug, H.J. 1997. The age and tectonic significance of dolerite dykes in western Norway. *Journal of the Geological Society, London*, **154**, 961–973, http://doi.org/10.1144/gsjgs.154.6.0961

van der Pluijm, B.A., Hall, C.M., Vrolijk, P.J., Pevear, D.R. & Covey, M.C. 2001. The dating of shallow faults in the Earth's crust. *Nature*, **412**, 172–175.

Wain, A. 1997. New evidence for coesite in eclogite and gneisses: defining an ultrahigh-pressure province in the Western Gneiss region of Norway. *Geology*, **25**, 927–930.

Wennberg, O.P., Milnes, A.G. & Winsvold, I. 1998. The northern Bergen Arc Shear Zone – an oblique-lateral ramp in the Devonian extensional detachment system of western Norway. *Norsk Geologisk Tidsskrift*, **78**, 169–184.

Wilson, T.J. 1966. Did the Atlantic close and then re-open? *Nature*, **211**, 676–681.

Woznitza, T. 2014. *Exhumation history of the Caledonides in SW-Norway – (U–Th)/He ages on apatite and K/Ar age determinations*. MSc thesis, University of Göttingen.

Young, D.J., Hacker, B.R., Andersen, T.B. & Gans, P.B. 2011. Structure and 40Ar/39Ar thermochronology of an ultrahigh-pressure transition in western Norway. *Journal of the Geological Society, London*, **168**, 887–898, http://doi.org/10.1144/0016-764920 10-075

Zwingmann, H. & Mancktelow, N. 2004. Timing of Alpine fault gouges. *Earth and Planetary Science Letters*, **223**, 415–425.

Zwingmann, H., Mancktelow, N., Antognini, M. & Lucchini, R. 2010. Dating of shallow faults: new constraints from the AlpTransit tunnel site (Switzerland). *Geology*, **38**, 487–490.